

Scan-rate-dependent Ion Current Rectification and Rectification Inversion in Charged Conical Nanopores

--Supporting Information--

*Dmitry Momotenko and Hubert H. Girault**

Laboratoire d'Electrochimie Physique et Analytique, Ecole Polytechnique Fédérale de Lausanne,
Station 6, CH-1015 Lausanne, Switzerland

RECEIVED DATE (to be automatically inserted after your manuscript is accepted if required according to the journal that you are submitting your paper to)

* CORRESPONDING AUTHOR FOOTNOTE

EMAIL: hubert.girault@epfl.ch

Telephone number: +41-21-693 3145

Fax number: +41-21-693 3667

SI-1. FEM Simulations Procedure

The FEM simulations were performed using the finite element software COMSOL Multiphysics (version 3.5a), operated on Linux Ubuntu 8.04 platform with a four Core Mac Pro 2.66 GHz CPU and 9.8 GB of RAM. As described previously,¹ the Nernst-Planck equations without electroneutrality and Poisson equation were solved using direct solver UMFPACK in transient form for the two-dimensional axisymmetric geometry of a nanopore (Figure SI-1). As shown on Figure SI-1, the computational is the conically shaped (half-cone angle $\alpha = 5^\circ$) axisymmetric channel of 5 μm length with the tip opening radius of 10 nm, placed between two equal reservoirs of solution. The size of the reservoirs and the length of the charged region outside the pore were adapted to have no influence on the results. Numerical solutions of NPP equations were obtained with the boundary conditions summarized in the Table SI-1.

Table SI-1. Boundary conditions for numerical simulations of ICR in conical nanopores. The numbers specifying the surfaces are correlated to the schematical representation of nanopore geometry shown on Figure 1 (\mathbf{n} denotes the vector normal to the surface).

Surface	Physical property	Boundary conditions	
		Nernst-Planck equations	Poisson equation
1	Equiconcentration, Equipotential	Concentration, $c_i = c_0$	Electric potential, $\phi = \phi_1$
2, 3, 7, 8	Insulating wall	Insulation, $-\mathbf{n} \cdot \mathbf{J}_i = 0$,	Zero charge, $\mathbf{n} \cdot (-\epsilon_0 \epsilon_r \nabla \phi) = 0$
4-6	Glass wall	Insulation, $-\mathbf{n} \cdot \mathbf{J}_i = 0$	Surface charge, $\mathbf{n} \cdot (-\epsilon_0 \epsilon_r \nabla \phi) = -\sigma$
9	Equiconcentration, equipotential	Concentration, $c_i = c_0$	Electric potential, $\phi = \phi_0$
10	Axial symmetry, z axis	Axial symmetry	Axial symmetry

Aqueous KCl solutions (with relative permittivity $\epsilon_r = 80$) at different bulk concentrations c were modeled assuming diffusion coefficients D_i of the ions $2.0 \cdot 10^{-9} \text{ m}^2 \cdot \text{s}^{-1}$ for both K^+ and Cl^- . The

nanopore (infinitely small wall thickness) carries the charge density $\sigma = -1 \text{ mC}\cdot\text{m}^{-2}$. The numerical solution of NPP equation system was computed, assuming room-temperature conditions with the following parameters: temperature $T = 298 \text{ K}$, $R = 8.31 \text{ J}\cdot\text{mol}^{-1} \cdot\text{K}^{-1}$ and vacuum permittivity $\varepsilon_0 = 8.854\cdot 10^{-12} \text{ F}\cdot\text{m}^{-1}$. The mesh was refined down to the value of 0.5 nm at the charged wall regions that should be enough to resolve features of diffuse double layer. In the present study we define the value of applied bias as potential difference between two electrodes, specified as surfaces 1 and 9 in Figure SI-1, *i.e.* $\Delta\phi = \phi_1 - \phi_9$. The value of ϕ_1 was given as $\phi_1 = \phi_0 - vt$ (ϕ_0 denote the Galvani potential ϕ_1 at $t = 0$ and equal to 0.6 V), while ϕ_9 was kept constant and equal to 0 V. Consequently, the Galvani potential difference could be described as $\Delta\phi = \phi_1 - \phi_9 = (\phi_0 - \phi_9) - vt = \Delta\phi_0 - vt$.

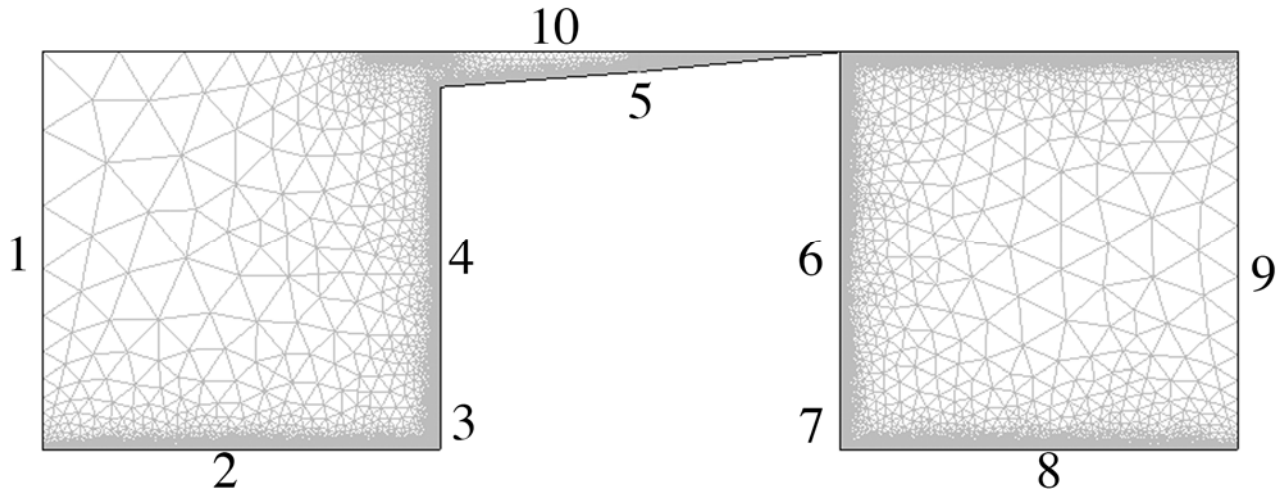


Figure SI-1. Schematic representation of a simulated axisymmetric model of the nanopore and the mesh used for computations. The numbers specify the surfaces with boundary conditions, described in Table SI-1.

SI-2. Validation of transient computations by comparison between solutions of steady-state and transient solvers at 1 V s^{-1} .

The comparison between steady-state ($\frac{\partial J_i}{\partial t} = 0$) and transient solutions at 1 V s^{-1} is a very important issue for validation of numerical results. The calculated values of rectification factors are shown on

Figure SI-2. As can be seen, the values calculated in pure steady-state conditions and at 1 V s^{-1} are very close to each other (the difference does not exceed 0.43%) proving the validity of the present transient numerical approach.

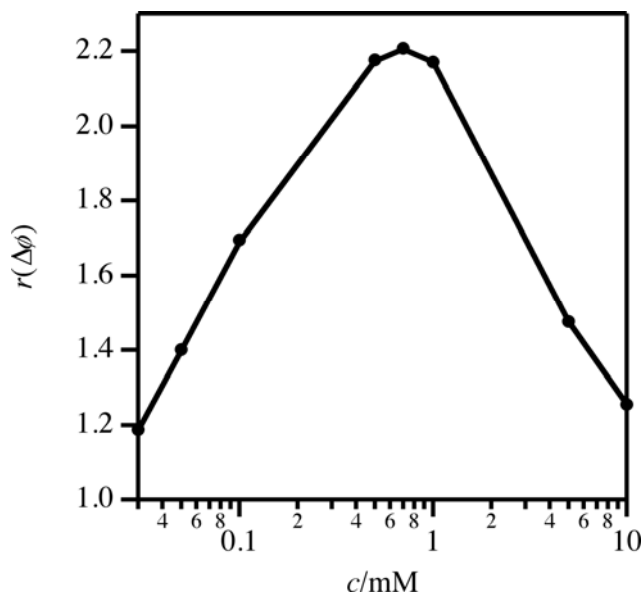


Figure SI-2. Calculated rectification ratio $r(\Delta\phi)$ using steady-state (dots) and transient solver at $v = 1 \text{ V s}^{-1}$ (solid line) at different bulk electrolyte concentrations c (given in a logarithmic scale).

SI-3. Effect of scan direction.

The scan direction could be modulated by varying ϕ_1 sign, *i.e.* applying $\phi_1 = -\phi_0 + vt$ as an electrical potential of the working electrode. The effect of the scan direction on rectification factors and the shape of current-voltage curves appears only at high potential scan rates. The resulting $i-V$ characteristics shown on Figure SI-3 has similar shape to ones reported by Guerrette *et al.*,² however, the magnitude of the effect is relatively small compared to the experimental results. As can be seen from Figure SI-3a, when the voltage scan is directed from positive to negative values the corresponding current-voltage curve is concave in quadrant I and convex in quadrant III, while on the contrary the shape of the curve for the reverse scan is convex in quadrant I and concave in quadrant III. The similar $i-V$ characteristics of the nanopores were found experimentally.² Corresponding curves at “transition” domain (see Figure

SI-3 b) are less influenced by the scan direction.

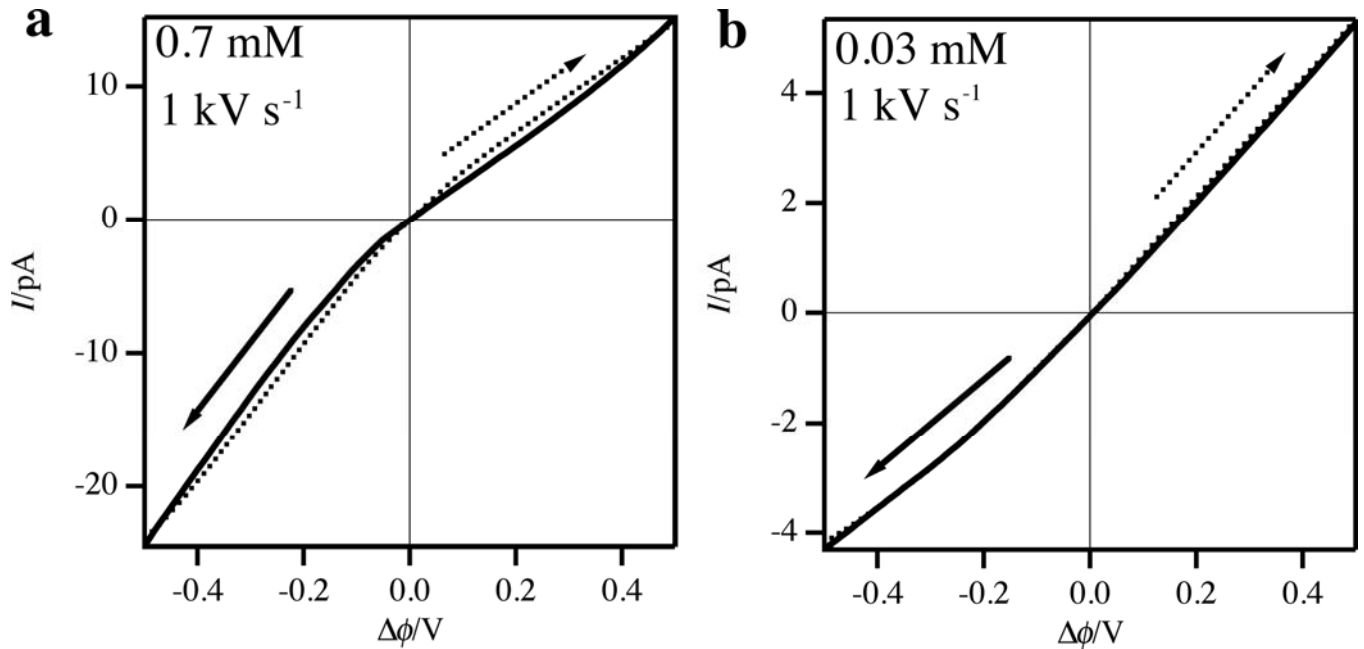


Figure SI-3. Current-voltage characteristics of conical nanopore at a) 0.7 mM and b) 0.03 mM KCl at scan rate $\nu = 1000 \text{ V s}^{-1}$ computed at different scan direction: an applied voltage scans from positive to negative values (solid lines) or from negative to positive (dotted lines). Arrows on the graph specify the scan direction for corresponding curves.

SI-4. Mass-transport by diffusion and migration at low (1 V s^{-1}) and high (1000 V s^{-1}) potential scan rates.

Figure SI-4 shows the rate of diffusion and migration components of ionic transport in the nanopore at different potential scan rates. As can be seen, at high scan rates the diffusional contribution to the total flux remains almost constant in a time scale of the voltage scan whereas migrational component of the current rectifies.

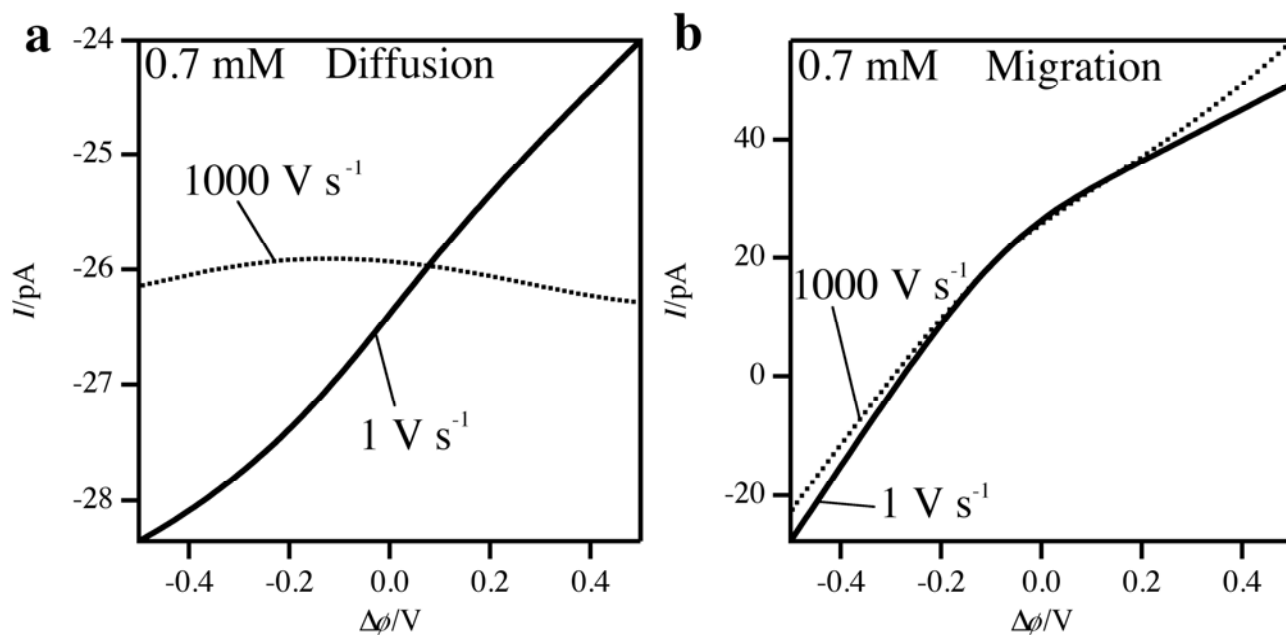


Figure SI-4. a) Diffusion and b) migration currents passing through the nanopore filled with 0.7 mM KCl at potential scan rate $\nu = 1 \text{ V s}^{-1}$ (solid lines) and $\nu = 1000 \text{ V s}^{-1}$ (dotted lines).

REFERENCES

- (1) Momotenko, D.; Cortes-Salazar, F.; Josserand, J.; Liu, S. J.; Shao, Y. H.; Girault, H. H. *Phys. Chem. Chem. Phys.* **2011**, *13*, 5430.
- (2) Guerrette, J. P.; Zhang, B. *J. Am. Chem. Soc.* **2010**, *132*, 17088.